ChemPubSoc Europe

DOI: 10.1002/open.201800011

Open Access ChemistryOPEN Full Papers

# Manufacturing Nanoparticles with Orthogonally Adjustable Dispersibility in Hydrocarbons, Fluorocarbons, and Water

Lukas Zeininger,[a] Lisa M. S. Stiegler,[a] Luis Portilla,[b] Marcus Halik,[b] and Andreas Hirsch*[a]

We describe a universal wet-chemical shell-by-shell coating procedure resulting in colloidal titanium dioxide ($TiO_2$) and iron oxide ($Fe_3O_4$) nanoparticles with dynamically and reversibly tunable surface energies. A strong covalent surface functionalization is accomplished by using long-chained alkyl-, triethylenglycol-, and perfluoroalkylphosphonic acids, yielding highly stabilized core–shell nanoparticles with hydrophobic, hydrophilic, or superhydrophobic/fluorophilic surface characteristics. This covalent functionalization sequence is extended towards a second noncovalent attachment of tailor-made nonionic amphiphilic molecules to the pristine coated core–shell nanoparticles via solvophobic (i.e. either hydrophobic, lipophobic, or fluorophobic) interactions. Thereby, orthogonal tuning of the surface energies of nanoparticles via noncovalent interactions is accomplished. As a result, this versatile bilayer coating process enables reversible control over the colloidal stability of the metal oxide nanoparticles in fluorocarbons, hydrocarbons, and water.

## 1. Introduction

Metal oxide nanoparticles exhibit unique size-related properties and have been implemented as central components of a large variety of electronic,[1,2] catalytic,[3] medical,[4,5] and performance materials.[6] With regard to their use in technological applications, major focus in nanoparticle research is directed towards 1) a generation of colloidal stability of the nanoparticles in solutions,[7] 2) directing their self-assembly into nanostructures,[8–10] and 3) controlling their wettability characteristics.[11,12] By using a chemical surface modification with organic molecular self-assembled monolayers (SAMs), the chemical and physical surface properties of thermodynamically unstable nano-sized particles can be controlled.[13] At the same time, most of the inherent material properties can be maintained. This is why most procedures for the synthesis of nanoparticles provide an in situ capping agent to sterically and/or electrostatically stabilize the newly formed nanocrystals.[14,15] However, a substitution of this stabilizing ligand shell in order to customize the surface properties of nanoparticles can be problematic as this can promote irreversible changes to the nanoparticles, including Ostwald ripening, which can ultimately lead to unwanted agglomeration and growth, causing a loss of the nanoparticles' special properties.[16] Approaches to circumvent these complications rely on a property management of the initial ligand capped nanoparticles. By modification of the existing ligand shell, the polarity of the nanoparticle surfaces can be reversed and colloidal stability in aqueous environments can be generated. Examples include a chemical modification of the ligand on the surface by chemical reactions (e.g. oxidations) or the establishment of an additional thin layer of inorganic or organic building blocks (e.g. with amphiphilic co-polymers).[17,18] However, despite its relevance, there is no generalizable route towards a switchable reversion of polarity of SAM-stabilized nanoparticles in various orthogonal solvents such as water, polar and apolar hydrocarbons, or superhydrophobic environments such as fluorocarbons. As such, a noncovalent self-assembly of small functional nonionic amphiphiles with pristine coated nanoparticles represents a very gentle and straightforward approach. This includes the introduction of new nanoparticle coating concepts, for example, employing amphiphilic fluorocarbons. At the same time, the scope of processability and practical application could be considerably broadened towards new options for the preparation of nanoparticle thin films as well as for the selective scavenging of amphiphilic components by core–shell colloids.

In this work, we introduce for the first time an entirely orthogonal tool kit for switchable nanoparticle functionalization. This concept relies on a combination of a strong covalent surface functionalization with noncovalent bilayer coating, using a set of amphiphiles with a permutation of terminal polarity, namely hydrophilic, lipophilic, and fluorophilic (Scheme 1). In a

[a] Dr. L. Zeininger, L. M. S. Stiegler, Prof. Dr. A. Hirsch
Department of Chemistry & Pharmacy
Friedrich Alexander University (FAU)
Henkestrasse 42, 91054 Erlangen (Germany)
E-mail: andreas.hirsch@fau.de

[b] Dr. L. Portilla, Prof. Dr. M. Halik
Department of Materials Science
Friedrich Alexander University (FAU)
Martensstrasse 9, 91058 Erlangen (Germany)

Supporting Information and the ORCID identification number(s) for the author(s) of this article can be found under https://doi.org/10.1002/open.201800011.

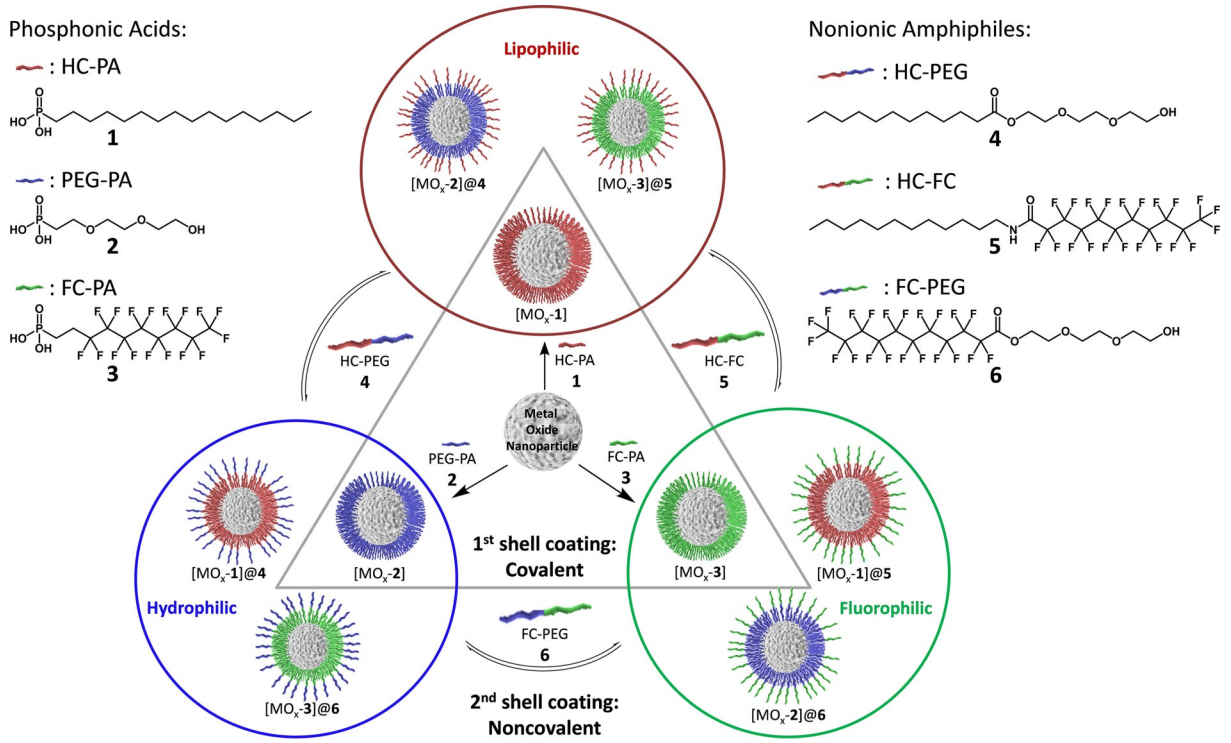


**Scheme 1.** Conceptional sketch of our orthogonal bilayer coating strategy. A combination of a strong covalent surface passivation of metal oxide nanoparticles with phosphonic acids **1**, **2**, and **3** and a subsequent noncovalent solvophobic interaction driven bilayer formation with amphiphiles **4**, **5**, and **6** leads to nanoparticles, which can reversibly adjust their surface energies resulting in colloidal stability in hydrocarbons, fluorocarbons and water.

first step, metal oxide nanoparticles ($MO_x$; namely titanium dioxide or iron oxide) were covalently functionalized in a wet-chemical functionalization approach with three different phosphonic acid derivatives, namely hexadecylphosphonic acid (HC-PA **1**), (2-(2-(2-hydroxyethoxy)ethoxy)ethyl)phosphonic acid (PEG-PA **2**), and (3,3,4,4,5,5,6,6,7,7,8,8,9,9,10,10,10-heptadecafluorodecyl)phosphonic acid (FC-PA **3**). Through this stable surface passivation, colloidal stability of the coated nanoparticles [$MO_x$-PA-HC], [$MO_x$-PA-PEG], and [$MO_x$-PA-FC] was achieved in hydrocarbons, water, and fluorocarbons, respectively. To reversibly tune the surface properties of these lipophilic, hydrophilic, and fluorophilic particles, and thus their dispersion behavior, we added new tailor-made nonionic amphiphilic molecules HC-PEG **4**, FC-PEG **5**, and HC-FC **6**. The key was a noncovalent solvophobic interaction-driven self-assembly of these amphiphilic molecules **4**–**6** with the shells of stable phosphonic-acid-functionalized nanoparticles [$MO_x$-1], [$MO_x$-2], and [$MO_x$-3]. As a result, this shell-by-shell coating approach allowed for the manufacturing of nanoparticles with orthogonally adjustable and switchable colloidal stability in hydrocarbons, fluorocarbons, and water.

## 2. Results and Discussion

A covalent surface modification of metal oxide nanoparticles with phosphonic acid derivatives has been proven to provide densely packed self-assembled monolayers on the nanoparticle surface displaying remarkable chemical stability.[19–21] As metal oxides, we used the commercially available starting materials $TiO_2$ nanoparticles and superparamagnetic $Fe_3O_4$ nanoparticles. The average diameter sizes were 34 and 15 nm, respectively. As for the wet-chemical surface functionalization, we sonicated 0.15 wt% suspensions of metal oxide nanoparticles in a 5.0 mm solution of HC-PA 1, PEG-PA 2, and FC-PA 3 in isopropanol, followed by centrifugation of the functionalized material in order to separate from non-surface-adsorbed organic molecules. The functionalized material was characterized by using thermogravimetric analysis (TGA), Fourier-transform infrared spectroscopy (FTIR), static contact angle (SCA), as well as dynamic light scattering (DLS) measurements (see the Supporting Information). Althoguh metal oxide nanoparticles functionalized with a monolayer of PEG-PA **2** were highly hydrophilic and, thus, dispersible in aqueous solutions, [$MO_x$-**1**] and [$MO_x$-**3**] readily sediment from polar solutions. The steric stabilization in [$MO_x$-**1**] provided lipophilic surface characteristics, rendering them well dispersible in apolar organic solvents such as toluene. Fluorinated metal oxide nanoparticles [$MO_x$-3] were nondispersible in both, water and toluene, but selectively dissolved in fluorocarbon solvents such as perfluoro(methylcyclohexane) (Figure 1).

Surfactant stabilization is a powerful technique for mixing and dispersing immiscible hydrophobic nanoparticles within a continuous aqueous phase.[22–24] As we demonstrated in a previous publication,[25] dispersions of nanoparticles coated with an alkyl-SAM can be functionalized with ionic as well as zwitterionic surfactants in water. To study this hydrophobic interaction driven self-assembly with nonionic surfactants, we synthesized a simple model amphiphile HC-PEG **4** to investigate its

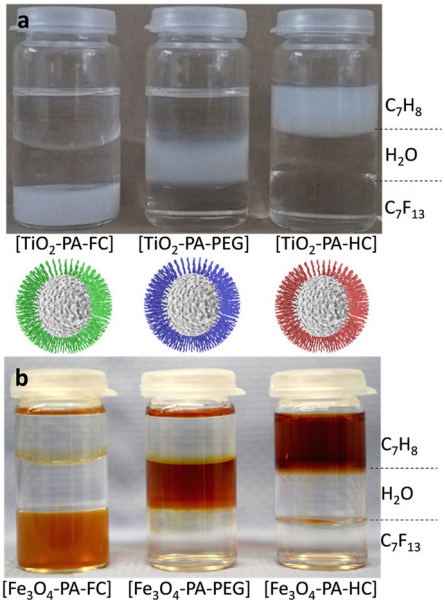


**Figure 1.** Dispersibility behavior of $TiO_2$ (a) and $Fe_3O_4$ (b) nanoparticle monolayers coated with HC-PA **1**, PEG-PA **2**, or FC-PA **3** when dispersed in a three-phase solvent system of toluene ($C_7H_8$), water ($H_2O$), and perfluoro(methylcyclohexane) ($C_7F_{13}$).

ability to increase the dispersibility of metal oxide nanoparticles coated with alkyl-phosphonic acid [$MO_x$-**1**]. The amphiphile HC-PEG **4** used in this study was synthesized through the esterification of lauric acid chloride **7** with triethylene glycol according to a modified literature procedure (Figure 2).[19] Com-

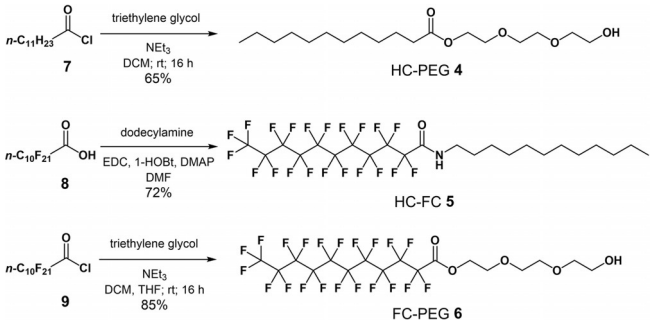


**Figure 2.** Synthetic procedures towards nonionic amphiphiles HC-PEG **4**, FC-PEG **5**, and HC-FC **6**.

pound **4** exhibits an alkyl moiety covalently linked to a glycol moiety and, thus, represents a simple nonionic hydrocarbon–water surfactant. We also sought to investigate whether this hydrophobic interaction driven self-assembly was transferrable to other particle-capping ligands as well as other solvent environments. Therefore, we synthesized amphiphiles HC-FC **5** and FC-PEG **6**, both consisting of a perfluorinated alkyl moiety covalently linked to either a hydrocarbon or a triethylene glycol moiety (Figure 2). HC-FC **5** was synthesized through 1-ethyl-3-(3-dimethylaminopropyl)carbodiimide (EDC) coupling of perfluorinated undecanoic acid **8** with dodecylamine yielding the respective amide in 72% yield. An esterification of perfluorinated undecanoic acid chloride **9** with triethylene glycol afforded **6** in 85% yield.

Upon addition of **4** to hexadecylphosphonic acid functionalized nanoparticles [$TiO_2$-**1**] in water, an immediate increase of the colloidal stability was noticeable. This stabilizing effect can be attributed to a hydrophobic interaction driven self-assembly of the hydrophobic tails of amphiphiles **4** with the hydrophobic ligand shell of the functionalized nanoparticle surfaces [$TiO_2$-**1**]. The particles act as nucleation sites for a formation of an orthogonal molecular bilayer around the nanoparticles. In such a micellar arrangement of the amphiphiles around the particle cores, the glycol moieties are pointing outwards, providing colloidal stability in polar solvents such as water. The extent of the electrosteric stabilization upon addition of amphiphiles **4** was characterized by using concentration-dependent zeta-potential measurements (Figure 3a). The zeta poten-

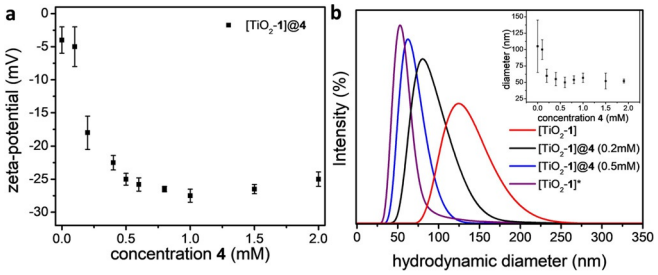


**Figure 3.** Concentration-dependent zeta-potential (a) and DLS (b) measurements of the bilayer coated nanoassemblies [$TiO_2$-1]@**4** in water. (*DLS of pure [$TiO_2$-1] in toluene). Uncertainty represents standard deviation of three measurements.

tial smoothly increased from slightly negative values for pure [$TiO_2$-**1**] of $\zeta = -5$ mV to $\zeta = -25$ mV upon stepwise addition of amphiphiles **4**. The formation of the bilayer coated structure led to the desirable electrosteric nanoparticle stabilization in solution. A concentration of 0.5 mm was sufficient to stabilize the 0.15 wt% nanoparticle dispersion in water.

In accordance with the zeta-potential measurements, DLS measurements of the same particle dispersions revealed a decreasing average hydrodynamic particle size upon addition of the stabilizing adlayer of **4** (Figure 3b). Although pure [$TiO_2$-**1**] rapidly formed large agglomerates in water, a dispersion of [$TiO_2$-**1**] in an aqueous solution of **4** (0.5 mm) resulted in single-particle-stabilized colloidal dispersions, as characterized by DLS. It is worth mentioning that, after centrifugation, the bilayer coated assemblies could be isolated as solids. The precipitates were re-dispersible in toluene (owing to the first-shell coating) as well as in water (bilayer coated material), indicating the adjustable surface energies through reversible formation of the second-shell structures. The solid material was further characterized by FTIR and TGA, which both supported the successful formation of the molecular bilayer structure (see the Supporting Information). The IR spectra of centrifuged and dried bilayer coated particles displayed characteristic vibrational bands of the phosphonic acids, which gave evidence that the phosphonic acid ligands were indeed still bound to the metal

oxide surfaces. In the TGA weight-loss curves of the bilayer coated structures, the weight loss of **4** was observed in addition to the weight-loss step of covalently bound phosphonic acid **1**. The noncovalent nature of the second-shell binding further resulted in desirable features such as reversibility (solubility in water and toluene) and exchangeability (exchange against other amphiphilic molecules). Demonstration experiments to prove that second-shell amphiphiles were easily exchangeable, but, once formed, assembled in close proximity to the particle core, were conducted by employing fluorescent marker amphiphiles **10** (Figure 4a).[25] Colored assemblies of

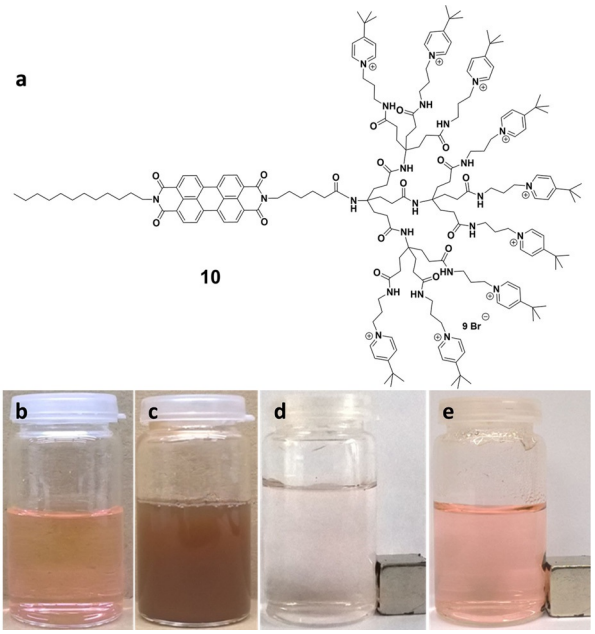


**Figure 4.** a) Structure of colored amphiphiles **10**; b) a solution of **10** in water and c) the same solution after addition of [$Fe_3O_4$-**1**] and sonication; d) the solution becomes transparent upon magnetic extraction of the bilayer functionalized nanoparticles to the sidewall of the glassware for 24 h; e) the same solution upon addition of competing amphiphiles in excess, sonication, and magnetic removal of $Fe_3O_4$ nanoparticles from solution.

functionalized titanium oxide particles [$TiO_2$-PA-HC] with fluorescent amphiphiles **10** became colorless upon centrifugation and re-dispersion in a solution of competing amphiphiles (Figure S6). By using hydrophobically coated superparamagnetic [$Fe_3O_4$-**1**] nanoparticles as scavengers, this mechanic extraction could be extended towards a magnetic removal of amphiphiles **10** from aqueous solution (Figure 4b–e). Interestingly, upon re-dispersion and addition of competing amphiphiles in excess, the second-shell ligands were replaced, leading to a release of **10** into water. This facile exchange of the second-shell functionality gave further evidence of the reversibility of our supramolecular binding concept.

The pronounced stability of the bilayer coated structures enabled the fabrication of spray-coated films of the nanoparticle assemblies on $SiO_2$ wafers. The self-assembled structures were sufficiently stable to demonstrate the variations of the surface energies through static contact angle experiments. In one of the most striking examples, we added nonionic amphiphiles **6** to an aqueous dispersion of [$TiO_2$-**3**]. Similar to the self-assembly of hydrocarbon-surfactant **4** with [$TiO_2$-**1**], an increase of particle dispersibility upon addition of **6** was immediately observed. Figure 3a displays an image of the fluoroalkyl-functionalized nanoparticles [$TiO_2$-**3**] dispersed in pure water and a 0.5 mm aqueous solution of FC-PEG **6**. Freshly prepared spray-coated films of the nanoparticle assemblies demonstrated the large variations of the static contact angles of water droplets on these surfaces. Although spray-coated films of [$TiO_2$-**3**] exhibited superhydrophobic properties with a static contact angle of water $\Theta > 160^\circ$, a pre-treatment of these pristine coated nanoparticles [$TiO_2$-**3**] with amphiphiles **6** to form the bilayer coated structures and a subsequent spray coating of [$TiO_2$-**3**]@**6** revealed a static contact angle of water of $\Theta < 20^\circ$ (see images in Figure 3a). The hydrophobic-interaction-driven self-assembly of the perfluorinated side chains of amphiphiles **6** with the fluorinated SAM of [$TiO_2$-**3**] was further monitored by DLS and zeta-potential measurements (see the Supporting Information) as well as by UV/Vis spectroscopy (Figure 5b).

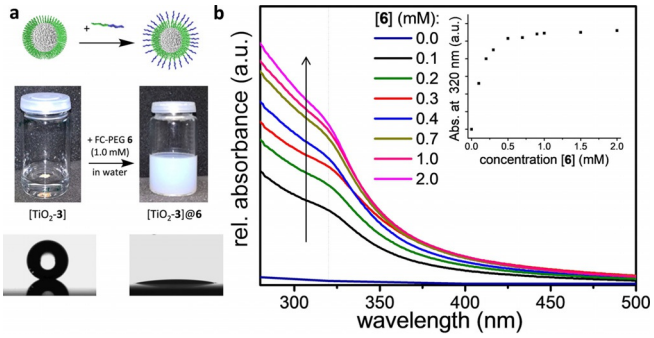


**Figure 5.** a) Images of [$TiO_2$-**3**] in water before and after addition of stabilizing amphiphiles **6**, and images of a water droplet on the surface of spray-coated films of [$TiO_2$-**3**] and [$TiO_2$-**3**]@**6**. b) UV/Vis spectra of the particle dispersions in water and increase of the $TiO_2$ band-gap absorption in the solutions upon stepwise addition of amphiphiles **6**, owing to enhanced colloidal stability.

Here, we monitored the increasing band-gap absorption of the $TiO_2$ nanoparticles at $\lambda = 320$ nm of dispersions of [$TiO_2$-**3**] in water as a function of the added concentrations of **6**. The measurements supported our findings that concentrations of $> 0.5$ mm led to a full bilayer structure formation and, thus, colloidal stability of [$TiO_2$-**3**] in water. In another experiment, we monitored the temperature-dependent zeta potential of such nanoassemblies (Figure S5). It was found that the molecular bilayer self-assembled structure was stable over a wide temperature range up to the boiling point of water.

The hydrophobic interaction-driven reversion of polarity upon the addition of nonionic amphiphiles can also be readily applied and generalized towards a solvophobic, in our case a lipophobic and a fluorophobic, interaction-driven self-assembly. Consistent with our previous experiments, a self-assembly of fluorinated nanoparticles [$TiO_2$-**3**] with hydrocarbon–fluorocarbon amphiphiles **5** led to an increase of the particle dispersibility when dispersed in a hydrocarbon solvent (toluene), whereas addition of the same amphiphile **5** to a colloidal sus-

pension of [$TiO_2$-**1**] resulted in stable colloidal suspension in perfluoromethylcyclohexane. Similarly, the solvent repellency of [$TiO_2$-**2**] when dispersed in lipophilic or fluorophilic media decreased upon addition of amphiphiles **4** or **6**, respectively. In addition to monitoring the self-assembled structure formation using DLS and UV/Vis techniques, measurements of the static contact angles of three solvents (water, diiodomethane, and *n*-hexadecane) on spray-coated films of these assemblies allowed for the calculation of the surface energies of all mono- and bilayer coated nanoparticles. The results of these measurements, which are displayed in Figure 6 (details in the Supporting Information), show that the surface energies of pristine coated nanoparticles [$MO_x$-PA-HC], [$MO_x$-PA-PEG], and [$MO_x$-PA-FC] were (statistically) significantly changed upon addition of nonionic amphiphiles **4**–**6**. These findings gave final evidence that the presence of simple nonionic amphiphilic molecules can successfully decrease the interfacial tensions of stable precoated nanoparticles when dispersed in orthogonal solvents.

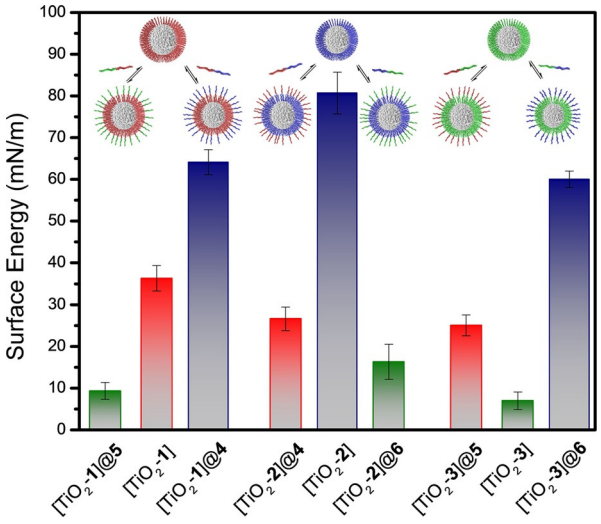


**Figure 6.** Surface energies of the mono- and bilayer coated nanoparticle assemblies (amphiphiles concentration in solution: 1.0 mm) calculated from the average static contact angles of water, diiodomethane, and *n*-hexadecane on spray-coated thin films of the nanoparticle assemblies.

## 3. Conclusions

The combination of a strong covalent surface passivation and a noncovalent, dynamic, and reversible self-assembly of amphiphiles with pristine coated nanoparticles led to nanoparticles that reversibly adjust their surface energies to certain solvent environments, yielding colloidal stability that can be reversibly alternated between hydrocarbons, water, and fluorocarbons. In addition to this highly practical application of reversible nanoparticle dispersibility, this orthogonal tool kit for a switchable nanoparticle functionalization was applied for 1) a selective magnetic or mechanic scavenging of amphiphilic components from solution and 2) preparation of particle thin films with smoothly tunable wettability characteristics. The presented method for the generation of bilayer coated particles and its dynamic mechanism are general. We envision this coating concept to facilitate technological processability of nanoparticles and enable research on bilayer coated particulate assemblies beyond the initial demonstrations described here such as a targeted preparation of particulate carriers that selectively entrap and release specific immiscible components.

## Experimental Section

### General Methods and Procedures

All reagents were purchased from commercial sources and used as received, unless stated otherwise. Titanium oxide (anatase) nanoparticles with a specific surface area (SSA) of 46 $m^2 g^{-1}$ were purchased from Nanograde (Stäfa, Switzerland) as a 20 wt% suspension in isopropanol. Iron oxide nanoparticles with an average particle diameter of 15 nm were purchased from Sigma–Aldrich as a 0.5 wt% suspension in water. The metal oxide nanoparticles were functionalized in a wet-chemical functionalization process in 0.15 wt% dispersions in isopropanol. To ensure full coverage, the particles were exposed to 5.0 mm solutions of phosphonic acids **1**–**3**.[19] The particles were functionalized in a volume of 25 mL, corresponding to approximately 30 mg nanoparticles. After adding the phosphonic acid, the dispersions were sonicated for 30 min. After functionalization, the mixture was centrifuged for 10 min (14 000 rpm). The functionalization included three washing steps. A washing step included re-dispersion of the particles in isopropanol followed up by another sonication step for 10 min and centrifugation. Finally, the particles were dried under vacuum or converted into the desired solvent for characterization or follow-up experiments, keeping the particle concentration constant (0.15 wt%). For noncovalent functionalization of the pristine coated metal oxide nanoparticles (second-shell coating), amphiphiles (**4**–**6**) were added in varying concentrations to the pre-functionalized nanoparticles [$MO_x$-PA**1**-**3**] in 0.15 wt% dispersions in either water, isopropanol, perfluoro(methylcyclohexane), or toluene. Amphiphiles **4**–**6** were synthesized according to the detailed procedures described below. The formation of homogenous dispersions in certain solvents indicated a successful coupling. For analysis, such as zeta-potential and DLS measurements as well as UV/Vis spectroscopy, the suspensions were further diluted to obtain 0.015 wt% dispersions of particles. To calculate the surface energies of the particle assemblies from the static contact angle, nanoparticle films were manually spray coated onto $Si/SiO_2$ wafers with a 100 nm thermal oxide layer. Before deposition of the films, the wafers were cleaned with a 5 min oxygen plasma treatment at 200 W at a pressure of 0.2 mbar (Pico, Diener electronic GmbH, Germany). During the spray-coating process, the substrate was heated to 100 °C on a hotplate. Static contact angles (SCA) were measured with a Dataphysics OCA 30 instrument (Data Physics Instruments GmbH, Germany). SCA measurements were investigated by using the sessile drop method, utilizing deionized water, diiodomethane, and *n*-hexadecane (1.0 μL) as probe liquids. More detailed information about the experimental procedures and methods used is given in the Supporting Information.

### Synthesis

2-(2-(2-Hydroxyethoxy)ethoxy)ethyl dodecanoate (**4**) and fluorescent perylene bisimide amphiphiles **10** were synthesized according to literature procedures.[26,27]

*N*-Dodecyl-2,2,3,3,4,4,5,5,6,6,7,7,8,8,9,9,10,10,11,11,11-henicosafluoroundecanamide (**5**): To an ice-cooled solution of perfluoro-*n*-undecanoic acid (282.05 mg, 0.5 mmol) in 20 mL dimethylformamide under a nitrogen atmosphere, 4-dimethylaminopyridine (122.17 mg, 1 mmol) was added. The resulting mixture was stirred for 10 min at 0 °C, and then 1-HOBt (135.13 mg, 1 mmol) was added. After stirring the mixture for 15 min, EDC (191.70 mg, 1 mmol) was added. Then, the mixture was stirred for 45 min at 0 °C. Finally, dodecylamin (278.04 mg, 1.5 mmol) was added and the full reaction mixture was stirred for 3 days while the mixture was warmed from 0 °C to room temperature. The solvent was removed from the mixture under reduced pressure. The product was purified by column chromatography [eluent: cyclohexane/tetrahydrofuran (THF), 1:1, $R_f = 0.5$] to give 262 mg of a white crystalline solid in 72% yield.

$^1$H-NMR (400 MHz, [D$_8$]THF): $\delta = 0.89$ (t, 3H, $^3J = 7.2$ Hz, $CH_3$), 1.29–1.32 (m, 18H, $CH_2$), 1.55 (m, 2H, $CH_2$), 3.29 (dt, 2H, $^4J = 6.8$ Hz, C(O)NH–$CH_2$–), 8.55 (bs, 1H, NH) ppm. $^{13}$C-NMR (100 MHz, [D$_8$]THF): $\delta = 14.3$ (1C, $CH_3$), 23.4 (1C, $CH_2$), 27.5 (1C, $CH_2$), 29.8 (1C, $CH_2$), 30.0 (1C, $CH_2$), 30.2 (1C, $CH_2$), 30.4 (1C, $CH_2$), 30.5 (1C, $CH_2$), 30.6 (1C, $CH_2$), 32.7 (1C, $CH_2$), 35.0 (1C, $CH_2$), 40.5 (1C, NH–$CH_2$–), 111.7 (1C, $CF_3$), 119.4 (1C, $CF_2$), 125.8 (4C, $CF_2$), 128.7 (1C, $CF_2$), 138.1 (2C, $CF_2$), 152.6 (1C, –$CF_2$–CON–), 157.6 (1C, C=O) ppm. $^{19}$F-NMR (376 MHz, [D$_8$]THF): $\delta = -124.14$ (m, 2F, $CF_2$), −120.64 (m, 4F, $CF_2$), −119.67 (m, 10F, $CF_2$), −117.57 (t, 2F, $^3J = 15$ Hz, $CF_2$), −79.12 (t, 3F, $^3J = 13.2$ Hz, $CF_3$). FT-IR: $\nu$(N–H) 3341; $\nu$($CH_2$) 2957, 2918, 2847; $\nu$(C=O) 1692; $\rho$(C–H) 1472; $\nu$(C–F) 1204, 1144, 1082; $\rho$($CH_2$) 721 cm$^{-1}$. ESI-MS: *m/z* 749.2030 (M + $NH_4^+$). M.p.: 99.5 °C.

2-(2-(2-Hydroxyethoxy)ethoxy)ethyl-2,2,3,3,4,4,5,5,6,6,7,7,8,8,9,9,10,10,11,11,11-henicosafluoroundecanoate (**6**): Perfluoro-*n*-undecanoic acid chloride was dissolved in 15 mL dichloromethane (DCM) and 5 mL THF. To the reaction mixture, triethylene glycol (TEG, 0.65 mL, 4.84 mmol) and triethylamine (0.3 mL, 2.12 mmol) were added. The resultant solution was allowed to stir at room temperature overnight under a nitrogen atmosphere. The reaction mixture was diluted with DCM and washed successively with water (2×10 mL) and 0.5 N HCl (10 mL ×2), and finally dried over magnesium sulfate. The solvent was removed under reduced pressure and the crude product was purified by column chromatography (eluent: EtOAC/cyclohexane, 4:1, $R_f = 0.35$) to give **6** in 85% yield.

$^1$H-NMR (400 MHz, [D$_8$]THF): $\delta = 2.75$ (bs, 1H, OH), 3.45–3.48 (m, 2H, $CH_2$), 3.53–3.62 (m, 6H, $CH_2$), 3.71–3.78 (m, 2H, $CH_2$), 4.52–4.55 (m, 2H, $CH_2$) ppm. $^{13}$C-NMR (100 MHz, [D$_8$]THF): $\delta = 62.1$ (1C, –*O*–$CH_2$–$CH_2$–*O*–), 67.9 (1C, –*O*–$CH_2$–$CH_2$–*O*–), 68.6 (1C, –*O*–$CH_2$–$CH_2$–*O*–), 68.9 (2C, –*O*–$CH_2$–$CH_2$–*O*–), 71.3 (1C, –*O*–$CH_2$–$CH_2$–*O*–), 73.9 (1C, –*O*–$CH_2$–$CH_2$–*O*–), 109.0 109.3, 111.4, 111.7, 116.6 (10C, $CF_2$), 158.5 (1C, C=O) ppm. $^{19}$F-NMR (376 MHz, [D$_8$]THF): $\delta = -124.15$ (m, 2F, $CF_2$), −120.75 (m, 4F, $CF_2$), −119.64 (m, 10F, $CF_2$), −116.82 (m, 2F, –$CF_2$–COO–), −79.16 (t, 3F, $^3J = 13.2$ Hz, $CF_3$) ppm. FT-IR: $\nu$(O–H) 3412; $\nu$($CH_2$) 2940, 2872; $\nu$(C=O) 1778; $\nu$(C–F) 1202, 1146, 1072 cm$^{-1}$. ESI-MS: *m/z* 697.04856 (M + $H^+$), 714.07481(M + $NH_4^+$). M.p.: 46 °C.

## Acknowledgements

*Financial support from the Cluster of Excellence "Engineering of Advanced Materials" (EAM), funded by the German Research Council (DFG), and the Graduate Schools "Advanced Materials and Processes" (GSAMP) and "Molecular Science" (GSMS) is gratefully acknowledged.*

## Conflict of Interest

*The authors declare no conflict of interest.*

**Keywords:** amphiphiles · colloidal stability · nanoparticles · surface energy · surfactants

[1] X. Chen, S. S. Mao, *Chem. Rev.* **2007**, *107*, 2891 – 2959.
[2] M. Grätzel, *Inorg. Chem.* **2005**, *44*, 6841 – 6851.
[3] Y. Lan, Y. Lu, Z. Ren, *Nano Energy* **2013**, *2*, 1031 – 1045.
[4] L. H. Reddy, J. L. Arias, J. Nicolas, P. Couvreur, *Chem. Rev.* **2012**, *112*, 5818 – 5878.
[5] M. M. Alvarez, J. Aizenberg, M. Analoui, A. M. Andrews, G. Bisker, E. S. Boyden, R. D. Kamm, J. M. Karp, D. J. Mooney, R. Oklu, *ACS Nano* **2017**, *11*, 5195 – 5214.
[6] A. Weir, P. Westerhoff, L. Fabricius, K. Hristovski, N. Von Goetz, *Environ. Sci. Technol. Environ. Sci. Technology* **2012**, *46*, 2242 – 2250.
[7] D. Segets, R. Marczak, S. Schäfer, C. Paula, J.-F. Gnichwitz, A. Hirsch, W. Peukert, *ACS Nano* **2011**, *5*, 4658 – 4669.
[8] S. Mann, W. Shenton, M. Li, S. Connolly, D. Fitzmaurice, *Adv. Mater.* **2000**, *12*, 147 – 150.
[9] J. Hühn, C. Carrillo-Carrion, M. G. Soliman, C. Pfeiffer, D. Valdeperez, A. Masood, I. Chakraborty, L. Zhu, M. Gallego, Z. Yue, *Chem. Mater.* **2017**, *29*, 399 – 461.
[10] A. K. Boal, F. Ilhan, J. E. DeRouchey, T. Thurn-Albrecht, T. P. Russell, V. M. Rotello, *Nature* **2000**, *404*, 746 – 748.
[11] L. Portilla, M. Halik, *ACS Appl. Mater. Interfaces* **2014**, *6*, 5977 – 5982.
[12] S. Pan, A. K. Kota, J. M. Mabry, A. Tuteja, *J. Am. Chem. Soc.* **2013**, *135*, 578 – 581.
[13] S. P. Pujari, L. Scheres, A. Marcelis, H. Zuilhof, *Angew. Chem. Int. Ed.* **2014**, *53*, 6322 – 6356; *Angew. Chem.* **2014**, *126*, 6438 – 6474.
[14] J. M. Pettibone, D. M. Cwiertny, M. Scherer, V. H. Grassian, *Langmuir* **2008**, *24*, 6659 – 6667.
[15] M. Niederberger, *Acc. Chem. Res.* **2007**, *40*, 793 – 800.
[16] Y. Yin, A. P. Alivisatos, *Nature* **2005**, *437*, 664 – 670.
[17] V. Muhr, S. Wilhelm, T. Hirsch, O. S. Wolfbeis, *Acc. Chem. Res.* **2014**, *47*, 3481 – 3493.
[18] T. Pellegrino, L. Manna, S. Kudera, T. Liedl, D. Koktysh, A. L. Rogach, S. Keller, J. Rädler, G. Natile, W. J. Parak, *Nano Lett.* **2004**, *4*, 703 – 707.
[19] L. Zeininger, L. Portilla, M. Halik, A. Hirsch, *Chem. Eur. J.* **2016**, *22*, 13506 – 13512.
[20] M. Halik, A. Hirsch, *Adv. Mater.* **2011**, *23*, 2689 – 2695.
[21] S. A. Paniagua, A. J. Giordano, O. N. L. Smith, S. Barlow, H. Li, N. R. Armstrong, J. E. Pemberton, J.-L. Brédas, D. Ginger, S. R. Marder, *Chem. Rev.* **2016**, *116*, 7117 – 7158.
[22] C. Backes, C. D. Schmidt, F. Hauke, C. Böttcher, A. Hirsch, *J. Am. Chem. Soc.* **2009**, *131*, 2172 – 2184.
[23] J. Sjoblom, *Emulsions and Emulsion Stability*, CRC Press, Boca Raton, **2005**; Vol. 132.
[24] J.-H. Lee, Z. Cheglakov, J. Yi, T. M. Cronin, K. J. Gibson, B. Tian, Y. Weizmann, *J. Am. Chem. Soc.* **2017**, 139, 8054 – 8057.
[25] L. Zeininger, S. Petzi, J. Schönamsgruber, L. Portilla, M. Halik, A. Hirsch, *Chem. Eur. J.* **2015**, *21*, 14030 – 14035.
[26] R. Neissner, *Fette, Seifen, Fette Seifen Anstrichm.* **1978**, *80*, 303.
[27] J. Schönamsgruber, B. Schade, R. Kirschbaum, J. Li, W. Bauer, C. Böttcher, T. Drewello, A. Hirsch, *Eur. J. Org. Chem.* **2012**, *2012*, 6179 – 6186.

Received: January 13, 2018
Version of record online March 5, 2018

 